Probing *R*-parity violating models of neutrino mass at the Fermilab Tevatron via top squark decays

Siba Prasad Das,[1,*] Amitava Datta,[1,†] and Monoranjan Guchait[2,‡]
[1]*Department of Physics, Jadavpur University, Calcutta-700032, India*
[2]*Department of High Energy Physics, Tata Institute of Fundamental Research, Homi Bhabha Road, Mumbai-400005, India*
(Received 20 October 2003; published 30 July 2004)

We have estimated the limiting branching ratio of the *R*-parity violating (RPV) decay of the lighter top squark, $\tilde{t}_1 \rightarrow l^+ d$ ($l = e$ or μ and d is a down-type quark of any flavor), as a function of the top squark mass ($m_{\tilde{t}_1}$) for an observable signal in the di-lepton plus di-jet channel at the Tevatron Run-II experiment with 2 fb^{-1} luminosity. Our simulations indicate that the lepton number violating nature of the underlying decay dynamics can be confirmed via the reconstruction of $m_{\tilde{t}_1}$. The above decay is interesting in the context of RPV models of neutrino mass where the RPV couplings (λ'_{i3j}) driving the above decay are constrained to be small ($\lesssim 10^{-3}$–10^{-4}) by the measured values of the neutrino oscillation parameters. If $\tilde{t}_1$ is the next lightest super particle—a theoretically well motivated scenario—then the RPV decay can compete with the *R*-parity conserving (RPC) modes which also have naturally suppressed widths. The model independent limiting branching ratio can delineate the parameter space in specific supersymmetric models, where the RPV decay is observable and predicts the minimum magnitude of the RPV coupling that will be sensitive to Run-II data. We have found it to be in the ballpark value required by models of neutrino mass, for a wide range of $m_{\tilde{t}_1}$. A comprehensive future strategy for linking top squark decays with models of neutrino mass is sketched.

DOI: 10.1103/PhysRevD.70.015009 PACS number(s): 11.30.Pb, 13.85.−t, 14.60.Pq, 14.80.Ly

I. INTRODUCTION

The minimal supersymmetric standard model (MSSM) [1] is a well motivated extension of the standard model (SM), which is free from several shortcomings of the latter. As of now, there is no experimental evidence either in favor of or against it. Unfortunately, the mechanism of supersymmetry (SUSY) breaking is not known yet, although several interesting suggestions exist [1]. As a result there is no guideline for predicting the mass splitting between a SM particle and its superpartner and consequently, there is no theoretical information about the range of superparticle (sparticle) masses. There are some experimental lower bounds from unsuccessful collider searches at LEP [2] and Tevatron Run-I [3,4].

Currently the Run-II of the Tevatron (referred to hereafter as Run-II) is in progress. It is expected to deliver an integrated luminosity of at least 2 fb^{-1} per experiment at 2 TeV center-of-mass energy, which is more than one order of magnitude larger than the acquired luminosity in Run-I with center-of-mass energy 1.8 TeV. However, in view of the existing limits on the masses of the strongly interacting sparticles (squarks and gluinos) [2,3] and the rather marginal increase in center-of-mass energy, most of the unexplored parameter space in this sector is likely to be beyond the kinematic reach of Run-II as well. Yet this is the only currently available machine for direct SUSY searches until the LHC starts.

In view of this, the top squark (the superpartner of the top quark) is somewhat special. It may be lighter than the other squarks and gluinos due to several reasons. First, the large top Yukawa coupling which controls the evolution of the soft-supersymmetry breaking masses of the left- and right-handed top squarks, $\tilde{t}_L, \tilde{t}_R$, via the renormalization group (RG) equations, tends to reduce these masses [1]. Moreover, because of the large top quark mass, the two weak states $\tilde{t}_L, \tilde{t}_R$ may mix very strongly leading to a relatively large splitting between the two physical mass eigenstates $\tilde{t}_1, \tilde{t}_2$ [5] (in our notation $m_{\tilde{t}_2} > m_{\tilde{t}_1}$). Interestingly, the mass of the lighter state $\tilde{t}_1$ may be even below the top mass. In fact, it is quite conceivable that in certain region of the SUSY parameter space it happens to be the next lightest supersymmetric particle (NLSP), the lightest neutralino $\tilde{\chi}_1^0$ being the lightest supersymmetric particle (LSP) by assumption in most *R*-parity (R_p) conserving models. It is therefore very important to fix up the strategies for isolating the top squark signal for all possible decay modes. Yet another motivation to look for a light top squark is that it seems to be preferred by electroweak baryogenesis [6].

In many studies the MSSM is assumed to be a R_p conserving (RPC) theory. The R_p is a discrete symmetry imposed on the MSSM to avoid the lepton and baryon number violating interactions in the Lagrangian which lead to rapid proton decay. If, however, either lepton or baryon number violation is allowed, such catastrophic decays can be avoided. This can be achieved by imposing either the so-called baryon parity or the lepton parity [7,8] conservation. The resulting theory, called *R*-parity violating (RPV) MSSM [9], is phenomenologically attractive since it has many novel predictions. From the theoretical point of view both RPC and RPV versions of the MSSM are on equal footing since both require additional discrete symmetries beyond the gauge symmetry.

*Electronic mail: spdas@juphys.ernet.in
†Electronic mail: adatta@juphys.ernet.in
‡Electronic mail: guchait@tifr.res.in

The SUSY signatures are determined by whether R parity is assumed to be conserved or not. Conservation of R parity implies that all SUSY decay chains end up in the $\tilde{\chi}_1^0$ which is stable and escapes the detector. Thus a typical SUSY signature is always accompanied by some amount of missing transverse energy ($\not{E}_T$). The R-parity violating interactions [9,10] on the other hand would allow the LSP, which is not necessarily the $\tilde{\chi}_1^0$, to decay into SM particles leading to distinct signals [11]. Yet another type of signal is the direct decay of sfermions, into two SM particles [10]. In view of the large production cross section of $\widetilde{t_1}\,\widetilde{t_1}^*$ pairs, the class of lepton number violating decays generically denoted by

$$\tilde{t}_1 \rightarrow l_i^+ d_j \tag{1}$$

is an attractive channel for searching RPV interactions at Run-II. Such decays are driven by the $\lambda'_{i3j}\, L_i Q_3\, \overline{D}_j^c$ term in the superpotential where L, Q, and D are, respectively, the lepton doublet, quark doublet, and down-singlet-type superfield, and i,j are generation indices.

In recent times RPV models have attracted special attention as they can provide viable models of neutrino mass (m_ν). The basic mechanism has been known for a long time [12]. RPV models violate the lepton number if the baryon number is assumed to be conserved. Thus lepton number violating Majorana neutrino masses may naturally arise in such models. The lepton number may be violated by bilinear terms [9] in the superpotential of the form $\mu_i L_i H_u$, where i is a generation index, μ_i is a mass parameter, L_i is a lepton doublet superfield, and H_u is a Higgs superfield containing the Higgs boson responsible for up-type quark masses. When one redefines the fields to obtain orthogonal mass eigenstates, the left-handed neutrinos acquire tree level Majorana masses through mixing with the neutralinos. Lepton number may also be violated by trilinear terms in the superpotential [9] $\lambda_{ijk}\, L_i L_j \overline{E}_k^c$, where i, j, k are generations indices, $\overline{E}_k$ is a singlet charged lepton superfield. Such couplings generate the self-energy type of diagrams for the neutrinos violating the lepton number by two units and eventually lead to neutrino masses at the loop level.

The interest in this model has been revived after the atmospheric [13] and the solar neutrino [14] experiments confirmed that the neutrinos are not massless. Parameters of these models have been constrained by many groups using neutrino data [15,16]. The actual set of bilinear and trilinear couplings and their precise magnitudes required to explain the neutrino data is model dependent. However, some couplings belonging to the class λ'_{i3j} are important ingredients of model building. Considering a variety of models it has been shown, e.g., in Ref. [16], that the important couplings λ'_{i33}, for all i, turn out to be generically small ($\lesssim 10^{-3} - 10^{-4}$, depending on the magnitude of the soft breaking parameters in the RPC sector). This is certainly much stronger than the constraints obtained prior to the neutrino data [17]. Thus RPV decays of the top squark driven by these couplings may provide an avenue for probing the models of ν mass [18–20] at colliders.

In this paper we focus our attention on two interrelated topics:

(1) The viability of observing direct top squark decays through the lepton number violating channels, Eq. (1), at the upgraded Tevatron collider in a model-independent way using the event generator PYTHIA [21]. This is an issue important in its own right irrespective of models of ν mass.

(2) The implications of observation/nonobservation of this decay channel for models of neutrino mass.

The collider signatures, however, crucially depends on whether the top squark is the NLSP or not. If the top squark is not the NLSP and the RPV couplings are as small as that required by the models of the neutrino mass, it would dominantly decay via the RPC two-body mode with nearly 100% branching ratio (BR) [22,23],

$$\tilde{t}_1 \rightarrow b \tilde{\chi}_1^+, \tag{2}$$

where $\tilde{\chi}^+{}_1$ is the lighter chargino. If the above mode is not kinematically allowed then it decays via the three-body modes [24],

$$\tilde{t}_1 \rightarrow b \ell \tilde{\nu},\;\; b \tilde{\ell} \nu,\;\; b W \tilde{\chi}_1^0, \tag{3}$$

where $\tilde{\ell}$ and $\tilde{\nu}$ are respectively the slepton and the sneutrino assumed to be lighter than $\widetilde{t_1}$. The decay of the LSP would then be the only signature of RPV interactions. Whether the magnitude of the underlying RPV coupling does indeed have the right ballpark value required by models of neutrino mass or not can be tested in principle, e.g., by measuring the width of the LSP. This, however, may not be an easy task at least in the Run-II experiments. In some models with small bilinear couplings the neutrino masses are dominantly generated by the trilinear couplings λ'_{i33}, where i is the lepton generation index. Thus the decay patterns of the LSP may give some circumstantial evidence in favor of/against models of neutrino mass. For example, if $\tilde{\chi}_1^0$ is assumed to be the LSP, then $\tilde{\chi}^+{}_1 \tilde{\chi}^-{}_1$ and $\tilde{\chi}^+{}_1 \tilde{\chi}_1^0$ production followed by decay chains involving the decays

$$\tilde{\chi}_1^0 \rightarrow \nu_\mu b \overline{b},\;\; \nu_\tau b \overline{b} \tag{4}$$

is indicative of an underlying model of neutrino mass [25]. In Ref. [25] the prospect of observing this signal at Run-II was studied. It was concluded that this signature can be probed up to $m_{1/2} = 230$ GeV (320 GeV) with an integrated luminosity of 2 fb^{-1} (30 fb^{-1}). Here $m_{1/2}$ is the common gaugino mass at the GUT scale. It is, however, worth noting that since the signal has missing energy carried by the neutrinos, it can be mimicked even if R parity is conserved. For example, the decay $\tilde{\chi}_2^0 \rightarrow \tilde{\chi}_1^0 b \overline{b}$, which may have a large BR if one of the bottom squark mass eigenstates happens to be lighter at large $\tan\beta$, has collider signatures very similar to the decay of Eq. (4). Moreover, the lepton number violating nature of the underlying interaction is not obvious since the neutrinos escape the detector. The possibility of probing RPV models of neutrino mass through neutralino decays has also been considered in Ref. [26].

The situation is totally different if the lightest neutralino and the top squark happen to be the LSP and the NLSP, respectively, a theoretically well motivated scenario for reasons discussed above. In this scenario the main RPC decay channels occur via the flavor changing neutral current decay mode [22],

$$\tilde{t}_1 \rightarrow c\tilde{\chi}_1^0, \tag{5}$$

and via four-body decay modes with a b quark, $\tilde{\chi}_1^0$, and two massless fermions [27],

$$\tilde{t}_1 \rightarrow b\tilde{\chi}_1^0 f\overline{f'} \tag{6}$$

(f and $\overline{f'}$ being a quark-antiquark or l-$\overline{\nu_l}$ pair) which eventually lead to RPV signals due to the LSP decay. Here the key point is that the above channels have widths suppressed due to natural reasons and can very well compete with each other [27] or with the direct RPV decay mode even, if the coupling λ'_{i3j} is $\sim 10^{-3}$–10^{-4}. As we shall see in a later section such competitions occur naturally over a large region of the MSSM parameter space. In fact if the above coupling is much larger then the direct lepton number violating decay mode Eq. (1) will occur with 100% BR's. The coexistence of the direct lepton number violating decay mode as well as RPC decay modes followed by the LSP decay, is a hallmark of RPV models of neutrino mass. Moreover, this signal is attractive due to the large production cross section of top squark pairs ($\tilde{t}_1\,\tilde{t}_1{}^*$). In addition, if a signal is observed then the underlying lepton number violating interaction can be revealed easily by reconstructing the top squark mass as will be illustrated in a later section. In the context of high Q^2 events at HERA [28] the signatures of this direct RPV decay at the Tevatron was first discussed in Ref. [29].

Obviously the presence of competing channels may complicate the search for the top squark. For example, if each of the competing modes has BR's substantially smaller than 100% all of them may be below the observable level in spite of large production rate of $\tilde{t}_1\,\tilde{t}_1{}^*$ pairs. A complete discussion is not possible without full simulations of all possible signals, which is beyond the scope of this paper. We shall concentrate on the first task, namely to estimate the minimum BR of top squark decay in RPV channel, Eq. (1), required for the observation of the signal at Run-II. This will be discussed in a subsequent section.

In a recent paper it has been shown [20] that the data from Run-I of the Tevatron already restrict the BR of the decay, Eq. (1), to values significantly smaller than 100% in a model-independent way for a range of top squark masses (see Fig. 3 of Ref. [20]). Assuming specific model parameters, which fixes the BR's of all the competing channels, this BR exclusion can be translated into upper bounds on the corresponding RPV coupling (see Fig. 4 of Ref. [20]). It was found for the first time, albeit for small values of the top squark mass and rather limited regions of the MSSM parameter space, that the Run-I data were indeed sensitive to magnitudes of these couplings relevant for models of neutrino mass. Since the accumulated luminosity of Run-II is more than an order of magnitude larger, we feel encouraged to investigate the feasibility of obtaining similar constraints over a much larger region of the MSSM parameter space. It may be recalled that in the past Tevatron di-lepton data were used to constrain the squark and gluino masses in the context of RPV SUSY model [30].

The possibility of probing the RPV models of neutrino mass via the direct RPV decays of the top squark was also suggested in Refs. [18,19]. These works, however, differ from ours in several ways. In Ref. [18], which was the first attempt to confront Run-I data with models of neutrino mass, it was claimed that for values of RPV couplings favored by models of neutrino mass, the RPV decay of the top squark dominates over the loop decay for $m_{\tilde{t}_1} \lesssim 150$ GeV. In the absence of four-body decays this statement is correct for low $\tan\beta$ only. For high $\tan\beta$ the loop decay can overwhelm the RPV mode. For low $\tan\beta$, on the other hand, the four-body decay, Eq. (6), not considered in Ref. [18], may dominate over the RPV decay if $\lambda' \approx 10^{-3}$–10^{-4}. The SU(2) gaugino mass M_2 also plays an important role in determining the relative strengths of these competing modes. All these issues will be addressed in great details in a subsequent section. In Ref. [19] the RPV mode, Eq. (1), the loop decay Eq. (5), and several three-body decay modes [including those in Eq. (3)], were assumed to be the competing channels. However, no detailed simulation was carried out to estimate the sensitivity of the data to RPV couplings.

We have organized the paper as follows. In Sec. II, we shall describe a road map for obtaining a comprehensive search strategy for top squark and its consequences for models of ν mass and briefly review the current status of top squark search, especially when it happens to be the NLSP. In Sec. III, the details of the simulation leading to model independent limiting values of the BR ($\tilde{t}_1 \rightarrow l^+ d_j$), where $l = e$ or μ, sensitive to Run-II data will be presented as a function of $m_{\tilde{t}_1}$. In Sec. IV, we use the results of Sec. III to obtain upper limits on RPV couplings in specific models and to understand the systematics of the parameter space (i.e., delineating the regions where some of the competing modes dominate or several of them may co-exist). We summarize our results in Sec. V.

II. ROAD MAP FOR LINKING TOP SQUARK SEARCH WITH MODELS OF NEUTRINO MASS

Our first task is to assess the viability of observing the direct RPV decay, Eq. (1) at Run-II. For simplicity we shall as usual assume that the RPV couplings are hierarchical, i.e., one coupling of the type λ'_{13j} dominates over the others.

For the sake of definiteness our simulations will be restricted to the mode $\tilde{t}_1 \rightarrow e^+ d_j$. This decay is triggered by the trilinear RPV coupling $\lambda'_{13j}\, L_e Q_3 \overline{D}_j^c$ term in the superpotential [9], where $j = 1$–3 is a generation index for down-type quarks. In order to make our analysis as general as possible, we have not employed any particular jet tagging so that the conclusions are approximately valid for any j.[1]

Our conclusions are also approximately valid for the coupling $\lambda'_{23j} L_\mu Q_3 \overline{D_j^c}$. A small difference may arise due to the difference in the detection efficiencies of e and μ. However, since the leptons are highly central the difference is rather marginal. Our conclusions cannot be applied to the signal from the $\lambda'_{33j} L_\tau Q_3 \overline{D_j^c}$ term which requires a fresh simulation taking into account τ detection efficiency. We, however, feel that the simplest signal arising from the class of decays in Eq. (1) will be sufficiently informative for the first analysis using an event generator.

A systematic search strategy for the top squark or, in the absence of a signal, a comprehensive limit on $m_{\tilde{t}_1}$ in RPV MSSM, therefore depends on several steps. The first step is to estimate the model-independent minimum value of $\sigma(p\overline{p} \to \tilde{t}_1 \tilde{t}_1^*) * (\epsilon_{br})^2$ for an observable signal as a function of $m_{\tilde{t}_1}$, where $\epsilon_{br} = \mathrm{BR}(\tilde{t}_1 \to e^+ d_j)$. Using the well-known formula for $\sigma(p\overline{p} \to \tilde{t}_1 \tilde{t}_1^*)$, which is available up to next to leading order (NLO) [31], this bound can be translated into a lower limit on observable BR. Rather low values of ϵ_{br} can be probed for a wide range of $m_{\tilde{t}_1}$ and it is also possible to reconstruct $m_{\tilde{t}_1}$ with a reasonable accuracy at Run-II, as we shall see in the next section.

The observation of the direct RPV decay signal alone, though a stupendous achievement in its own right, will shed little light on models of neutrino mass (m_ν). As discussed in the Introduction the simultaneous observation of the signals arising from the RPC decays in Eqs. (5) or (6), followed by $\tilde{\chi}_1^0$ decay may strongly hint in favor of these models. The observability of these signals depend on two factors: (i) the BR's of the decays involved, and (ii) the acceptance efficiency of the cuts in distinguishing the signal from the background.

Assuming that the dominant RPV decay mode of $\tilde{\chi}_1^0$ in RPV models of ν mass is $\tilde{\chi}_1^0 \to b\overline{b}\nu_i$, $i=1,2,3$, the signal resulting from the loop decay [Eq. (5)] is

$$\tilde{t}_1 \to c\tilde{\chi}_1^0 \to cb\overline{b}\nu_i. \tag{7}$$

Therefore $\tilde{t}_1 \tilde{t}_1^*$ pair production is signaled by jets$+\not{E}_T$ with four b jets. Similarly, the four-body decay, Eq. (6), would cascade into

$$\tilde{t}_1 \to b\tilde{\chi}_1^0 f\overline{f'} \to bb\overline{b}\nu_i f\overline{f'}. \tag{8}$$

An excess of $\ell+$jets$+\not{E}_T$, $2\ell+$jets$+\not{E}_T$ or jets$+\not{E}_T$ events including several b jets would therefore indicate $\tilde{t}_1 \tilde{t}_1^*$ pair production in the framework of RPV SUSY model. The above signals are very similar to the ones discussed in Ref. [25], although the signal from the decay chain in Eq. (8) may have even more b jets. From the results of Ref. [25] one has reason to be optimistic that the large number of b jets would provide a visible signal if b tagging is really efficient ($\sim$50%).

Full simulations of the above two signals, which is beyond the scope of this paper, would lead to the estimated minimum BR of the loop decay and the four-body decay required for observable signals at Run-II as a functions of $m_{\tilde{t}_1}$. These along with the minimum BR for observable RPV signal (estimated in the next section in detail) will provide the basis for a model-independent approach to top squark search at Run-II in the context of RPV models of m_ν.

If the signal is seen in the direct RPV channel as well as in one or both of the competing channels, one can try to identify the allowed parameter space using the limiting BR and the reconstructed $m_{\tilde{t}_1}$. Since the estimates of the limiting BR corresponding to the signals in Eqs. (7) and (8) are not available at the moment, a complete job cannot be done. However, the BR's of the $\tilde{t}_1$ decays will be discussed in detail in Sec. IV with an aim to understand the systematics of the MSSM parameter space vis-à-vis these decays. Outlines of a future comprehensive program for linking $\tilde{t}_1$ decay signals with models of ν mass will also be sketched with illustrative examples in Sec. IV.

The other important issue is the prospect of unambiguously excluding a range of $m_{\tilde{t}_1}$ if no signal is seen. Here one encounters the complications due to possible presence of three competing decay modes in a large parameter space. In fact the current mass limits on $m_{\tilde{t}_1}$ in both RPC and RPV models are also not free from ambiguities.

The phenomenology of top squark search Tevatron experiments in different decay channels have been studied extensively in both RPV [18–20] and RPC [32–35] models. The unsuccessful search for the top squark at LEP and Tevatron Run-I experiments in both RPC [36] and RPV MSSM [37,38] have yielded important bounds. Here we shall focus on the scenario when the top squark is the NLSP.

It is to be noted that the most stringent limits in RPV as well as RPC models have often been derived by employing the model-dependent assumption that the top squark decays into a particular channel with 100% BR. For example, the most stringent bound in the context of RPC MSSM comes from Tevatron Run-I experiments which puts a lower limit on lighter top squark mass $m_{\tilde{t}_1} \gtrsim 119$ GeV for $m_{\tilde{\chi}_1^0} = 40$ GeV. The limit becomes weaker for higher value of $m_{\tilde{\chi}_1^0}$, e.g., $m_{\tilde{t}_1} \gtrsim 102$ GeV for $m_{\tilde{\chi}_1^0} = 50$ GeV [36]. In deriving these limits, it was assumed that the loop induced decay, Eq. (5) [22], occurs with 100% BR. Apparently this assumption is valid in a wide class of models if the $\tilde{t}_1$ state happens to be the NLSP. Since the production cross section of top squark pairs is dominantly via QCD and depends on its mass only, the above limits from Tevatron therefore seem to be fairly model independent, except for the dependence on $m_{\tilde{\chi}_1^0}$, which influences the efficiency of the selection cuts.

[1]The most important ingredients of RPV models of ν mass are λ'_{i33} all of which are constrained to be $\lesssim 10^{-3}$–10^{-4} (see, e.g., Ref. [16]). However, for $d_j = b$, b tagging can be efficiently employed to improve the signal/background ratio and our conservative conclusions may be further strengthened (see Sec. III for further comments).

However, as has been shown in Ref. [27], even if the top squark is the NLSP, its four-body decay, Eq. (6), may indeed compete with the above loop decay or may even overwhelm it in some region of parameter space. The above limits therefore require revision and new signal via the four-body decay channel should be looked for [35].

The most recent limit on the top squark mass ($m_{\tilde{t}_1} \gtrsim 122$ GeV) in the RPV MSSM comes from the CDF Collaboration [37] in the decay channel,

$$\tilde{t}_1 \to \tau^+ + b. \tag{9}$$

This limit is also derived on the basis of the above model-dependent assumption, namely, the decay channel in question has a BR of 100%. However, even if the RPV coupling involved (λ'_{333}) is assumed to be the most dominant one, the mode may have a BR significantly smaller than 100%. This may happen in various regions of the MSSM parameter space simply due to the competition among this decay mode and the RPC modes of top squark, since the latter couplings are invariably present irrespective of the choice of the RPV sector. As discussed in the introduction the competition is of special interest, if the top squark is the NLSP and RPV couplings have strengths relevant for the models of neutrino mass [15,16]. In Ref. [20], on the other hand, the possibility of competition among different decay channels were considered. The mass limits obtained in Ref. [20] were naturally dependent on $\epsilon_{br} = \mathrm{BR}(\tilde{t}_1 \to e\bar{d})$. For example, it was found that $m_{\tilde{t}_1} \gtrsim 200$ (165) GeV for $\epsilon_{br} = 1$ (0.5).

If no RPV signal is seen at Run-II, any particular $m_{\tilde{t}_1}$ cannot be excluded in a model-independent way. Only the regions of the MSSM parameter space where the BR of at least one of the three competing decay modes is above the observable limit will be ruled out. On the other hand, one can also identify the difficult regions of the MSSM parameter space, in the context of Run-II, where all three decay modes have BR's below the corresponding observable limits. The stop search at LHC may focus on these regions. In such difficult regions the RPV signals from chargino/neutralino production followed by $\tilde{\chi}_1^0$ decay [25] appear to be the only possibility of probing models of ν mass at Run-II. Thus the top squark decay and the signal of Ref. [25] are essentially complementary in nature.

It should also be noted that the above top squark decay signals are important only if the top squark happens to be the NLSP, a scenario theoretically very well motivated but not inevitable. The signal of Ref. [25], on the other hand, requires the lighter chargino to be heavier than the $\tilde{\chi}_1^0$ which is not necessary in RPV models, unless gaugino mass unification [1] is assumed. Thus either of the above two signals, Eqs. (1) or (4), or both, may be helpful for probing RPV signals depending on the MSSM parameter space of interest.

The limit on the RPV BR in turn can be converted into upper limits on λ' in specific models with several competing channels. We shall demonstrate in Sec. IV that for a wide choice of model parameters magnitudes of λ' relevant for models of m_ν are expected to be sensitive to the data.

Once the LHC is in operation the signal size as well as the ability to probe smaller BR are expected to increase dramatically. The task of reconstructing $m_{\tilde{t}_1}$ and delineating the allowed/disfavored regions of the parameter space in specific models will be much easier. The program for a comprehensive top squark search will certainly take some time. Yet, it is gratifying to note that a systematic, largely model-independent strategy for top squark search in models of ν mass is quite possible in the not too distant future.

III. LIMITING VALUES OF BR($\tilde{T}_1 \to e^+ d$) FOR OBSERVABLE SIGNALS AT RUN-II

In hadron colliders, top squark pairs are produced via gluon-gluon fusion and quark-antiquark annihilation,

$$gg, q\bar{q} \to \tilde{t}_1 \tilde{t}_1^*. \tag{10}$$

The production cross section in the leading order depends only on mass of $\tilde{t}_1$ without any dependence on the mixing angle in the top squark sector, since it is a pure QCD process [40]. The total pair production cross section at the Tevatron for $\sqrt{s} = 2$ TeV is $\simeq 15$–0.3 pb which is 40% larger than the cross section for $\sqrt{s} = 1.8$ TeV, for the range of $m_{\tilde{t}_1} = 100$–200 GeV. The QCD corrections may enhance this cross section by $\sim 30\%$ over most of SUSY parameter space accessible at Tevatron [31].

We investigate the signal of top squark pair production in the channel e^+e^- plus two or more jets, assuming that both the top squark decays via a single RPV coupling λ'_{13j},

$$\tilde{t}_1 \to e^+ + d; \ \tilde{t}_1^* \to e^- + \bar{d}, \tag{11}$$

where we have suppressed the generation index of the d-type quark since we have not employed any specific flavor tagging.

The leading SM backgrounds corresponding to the signal with *opposite sign di-electron (OSDE) plus two or more jets* are the following:

a. Drell-Yan process via $q\bar{q}' \to e^+e^-$.
b. W boson pair production, $q\bar{q}' \to WW$, where both the W decay leptonically, $W \to e\nu_e$. Note that we also consider W decays to τ leptons which may decay to electrons.
c. $q\bar{q}' \to WZ$, where W decays hadronically and Z decays leptonically.
d. Z boson pair production also leads to the same final state: $q\bar{q}' \to ZZ \to (q\bar{q}')(ee)$.
e. Top quark pair production, $q\bar{q}, gg \to t\bar{t}$, where both the top quarks decay semi-leptonically via W, $t \to be\nu_e$.
f. Single top quark production, $q\bar{q}' \to tb$, where one lepton comes from top quark and the other comes from b-quark decay.
g. Tau pair production with both the τ decaying leptonically, i.e., $q\bar{q} \to \tau\bar{\tau} \to e^+e^-\nu_e\bar{\nu}_e$.

h. Bottom quark pair production $q\bar{q}\to b\bar{b}$ followed by fragmentation and hadronization of the b quarks. The leptons pair originates from the decay of B mesons.

In the above processes additional jets may come from initial/final state QCD radiation (ISR/FSR). We have analyzed the signal and the background processes using PYTHIA (v6.206) event generator [21]. We generate signal events in the di-electron+jets channel forcing $\tilde{t}_1$ to decay, $\tilde{t}_1\to e+q$ with 100% branching ratio switching off all other allowed decay modes of $\tilde{t}_1$ in PYTHIA.

In our calculation we set the renormalization and factorization scale to $Q^2=\hat{s}$ and use CTEQ3L [41] for the parton distribution functions. For the jet reconstruction we use the routine PYCELL in PYTHIA [21]. We selected events in the hadronic and electromagnetic calorimeter cells in pseudorapidity (η) and azimuthal angle (ϕ) of size $\Delta\eta\times\Delta\phi=0.1\times0.1$. Cells with $E_T>1$ GeV are taken as initial seeds to form calorimetric towers. Jets are reconstructed with cone radius 0.5 and only those are accepted which has transverse energy $E_T>8$ GeV and are smeared by $0.5\times\sqrt{E_T}$. We selected events applying the following set of cuts.

1. Leptons, required to be of opposite charges and of same flavor, are selected with $p_T^{\ell}>10$ GeV and $|\eta_\ell|<2.5$.
2. Number of jets is required to be $n_j\geqslant 2$, where, jets are selected if $E_T^j>15$ GeV, $|\eta_j|<3.0$. Isolation between any two jets is ensured by demanding $\Delta R(j,j)>0.5$, where $\Delta R=\sqrt{\Delta\phi^2+\Delta\eta^2}$.
3. Electrons and jets are assumed to be isolated, if $\Delta R(\ell,j)>0.5$.
4. Events with $80<M_{\ell\ell}<100$ GeV and $M_{\ell\ell}<10$ GeV are not accepted, where $M_{\ell\ell}$ is the di-electron invariant mass.
5. Azimuthal angle between two leptons are required to be $\phi(\ell\ell)<150°$.
6. Events are vetoed out for $\not{p}_T>25$ GeV.
7. The total visible energy of any event are required to be, $S_T>350$ GeV, where $S_T=H_T^{\ell}+H_T^{j}$; $H_T^{\ell(j)}=$scalar sum of transverse energy of all leptons (jets).
8. We constructed two lepton-jet invariant masses considering all possible combinations of the final state particles. Finally, we select only that combination in which the difference between two is minimum provided $|m(\ell_1 j_1)-m(\ell_2 j_2)|<20$ GeV.

Cuts 1–3 are basically event selection cuts. Cut 4 is used to suppress the backgrounds where lepton pair is coming from $Z\to\ell\ell$ decay. The aim of cut 5 is to suppress the background due to the Drell-Yan (DY) process (a) where leptons are mostly back to back in the azimuthal plane. Note that the signal is almost free from any missing momentum.[2] Therefore using cut 6 we vetoed out those events which involve a large amount of missing momentum. The background from WW and $t\bar{t}$ suffer heavily because of this cut. Finally, the cut on total visible energy, $S_T>350$ GeV, significantly reduces all backgrounds, particularly DY, to a negligible level, without costing too much in the signal cross section except for low values of $m_{\tilde{t}_1}$.

TABLE I. Results of the PYTHIA [21] simulation for all background processes for $\mathcal{L}=2$ fb^{-1}.

Process	Cross section (pb)	N_{1-6}	Efficiency (ϵ_k)	No. of events
WW	8.06	2	0.0	0.0
WZ	2.34	4	1.0×10^{-5}	0.047
ZZ	1.08	7	9.2×10^{-5}	0.199
$t\bar{t}$	4.38	6	3×10^{-5}	0.263
tq	2.39	0	0.0	0.0
DY	3.07×10^4	280	5×10^{-8}	2.959
$\tau\bar{\tau}$	2.97×10^4	10	0.0	0.0
$b\bar{b}$	3.570×10^7	0	0.0	0.0

In Table I, we summarize our results for all background processes assuming integrated luminosity 2 fb^{-1}. The second column contains the raw production cross section corresponding to each process. In the third column, we present the number of events (N_{1-6}) surviving after cuts 1–6. Finally, the effect of cut 7 is reflected in the last two columns where as in the fourth column we present the acceptance efficiencies for each of the processes due to the cuts N_{1-6} and in the last column the number of events survived by all sets of cuts are shown. We notice that the cuts N_{1-6}, mainly jet and lepton selection cuts, are very effective in eliminating the backgrounds due to gauge boson pair productions, as jets are not very hard in these processes. In the WW case, jets mainly arise due to ISR and are rather soft. As a result the selection efficiency turns out to be at the level of $\sim10^{-4}$ due to the jet selection cuts. On the other hand, in ZZ and WZ case, the lepton pair comes from Z decay, $Z\to ee$, where as the accompanying gauge boson decays hadronically. Therefore, although the jet selection cuts are less stringent in this case, cuts 4 and 5 are very effective. Similarly, $\tau\bar{\tau}$ and $b\bar{b}$ pair production suffer significantly due to the cuts, mainly lepton and jet selection cuts because of the facts that leptons in both the cases are very soft and those processes are hadronicaly quiet as well.[3] Recall that our signal is missing energy free, therefore vetoing events with missing energy, i.e., cut 6 is very effective to suppress the $t\bar{t}$ background enormously. Notice that all the background cross sections come down to negligible level due to the cuts N_{1-6} except the DY process. Finally, the cut on total visible transverse energy drastically reduce DY background bringing them to a negligible level along with other background process. Table I clearly shows

[2]Some amount of missing momentum may arise if jets or leptons go undetected due to loss in the beam pipe, for very low energies which are below the detection threshold or due to energy momentum mismanagement. In any case, the missing momentum is not so hard.

[3]Although some jets are expected from ISR/FSR, they rarely pass the selection cuts.

TABLE II. Results of the PYTHIA [21] simulation for the signal di-electron plus two or more jets due to the top squark pair production at Tevatron for $\mathcal{L}=2$ fb^{-1} luminosity

$m_{\tilde{t}_1}$ (GeV)	$\sigma(p\bar{p}\to\tilde{t}_1\tilde{t}_1^*)$ (pb)	N_{1-6}	Efficiency (ϵ_k)	No. of events	$S/\sqrt{B}$	Limiting BR (%)
80	28.09	18994	0.0056	314.6	168.93	17.2
100	8.59	6096	0.0194	333.3	178.97	16.7
120	3.18	2321	0.0473	300.8	161.53	17.6
140	1.34	993	0.0933	250.0	134.26	19.3
160	0.617	459	0.1566	193.2	103.76	21.9
180	0.304	227	0.2287	139.0	74.66	25.8
200	0.158	115	0.2798	88.41	47.47	32.4
220	0.084	60	0.3073	51.62	27.72	42.5
240	0.046	32	0.3206	29.49	15.83	56.2
260	0.026	17	0.2979	15.49	8.32	77.5

that our signal cross section is almost background free. The last criterion 8 is used to reconstruct top squark masses and to reveal the lepton number violating nature of the underlying interaction.

In Table II, which is of the same structure as Table I except for the last two columns, we show the signal characteristics for various top squark masses. Similarly, as before, columns 4 and 5 show the effect of cut 7 to the signal process. It is to be noted that the cut $S_T > 350$ GeV costs signal cross section heavily (by about factors of ~ 10–60) for lower values of $m_{\tilde{t}_1}(\lesssim 100$ GeV) as leptons and jets are relatively soft, where as for higher $m_{\tilde{t}_1}$ values this cut does not affect significantly. The signal efficiencies vary from ~ 2–30 % for the range of $m_{\tilde{t}_1}=100$–240 GeV. In column 6 we present the significance of the signal for $\epsilon_{br}=1$. The last column presents the minimum value of ϵ_{br} that can be measured at 5σ for an integrated luminosity of 2 fb^{-1}.

In Fig. 1 we show the minimum BR as a function $m_{\tilde{t}_1}$. The region above the solid line can be explored by Run-II for $\mathcal{L}=2$ fb^{-1}. In the same plane we show the region (above the dashed line) which is already excluded at 95% C.L. by Tevatron data [20]. Comparing the two regions we find that the improvement in sensitivity is by $\sim$ factor of 2–3 for 80 $\lesssim m_{\tilde{t}_1} \lesssim 160$ GeV. For higher top squark masses it is still

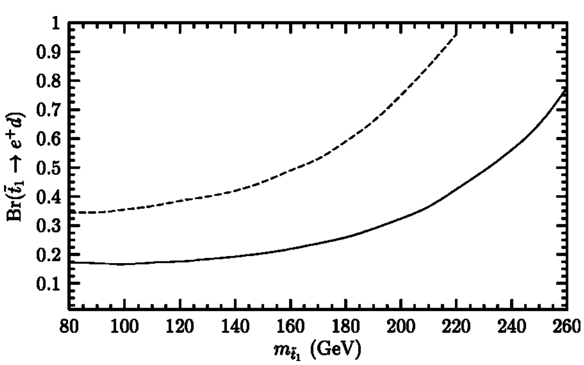

FIG. 1. The discovery region above the solid line for $\mathcal{L}=2$ fb^{-1} at Run-II. The region above the dashed line is excluded by Tevatron Run-I data [20].

quite significant. As discussed in Sec. II this is the first step for obtaining a model-independent search in the framework of RPV MSSM.

The actual limiting BR may be even smaller as can be seen, (i) by replacing the cross sections from PYTHIA (the second column of Table II) by the corresponding NLO cross sections of Ref. [31] which are typically larger by 30%, (ii) if accumulated luminosity significantly larger than 2 fb^{-1} is considered. Our results are therefore very conservative. More optimistic results can be easily obtained by dividing the limiting BR in Table I by $(\sigma_{NLO}/\sigma_p)^{1/2}$ $(\mathcal{L}_A/2\ \text{fb}^{-1})^{1/4}$, where σ_{NLO} is the cross section in Ref. [31], σ_p is the PYTHIA cross section, and $\mathcal{L}_A$ is the actual luminosity.

We have not tagged the flavor of any jet in the final state. We have checked that for $m_{\tilde{t}_1}=120$ (180) GeV the overall efficiency in Table II is reduced to 0.021 (0.097) (including a b-tagging efficiency of 50%) if d_j is identified with a b quark. This suppression, however, will be adequately compensated by strong reduction in the backgrounds. For example the Drell-Yan background will now be nonvanishing mainly due to misidentification of light quark and gluon jets as b jets, the probability of which is extremely small. Assuming the signal to be essentially background free and requiring ten events as the criterion for discovery, the limiting BR is found to be 27.3% (41.2%) for $m_{\tilde{t}_1}=120$ (180) GeV. Due to the uncertainties in cross section and $\mathcal{L}_A$ (see above) these limiting BR may be even smaller. We therefore feel that the numbers in Table II are fairly representative for all d-type flavors.

As we mentioned in the previous section, the limiting values of ϵ_{br} can also lead to constraints in the MSSM parameter space in RPV models of ν mass. We discuss them in detail in the next section. In these models the couplings λ'_{i33}, $i=1$–3, are the relevant ones in most scenarios. Considering di-leptons of the same flavor the BR in Fig. 1 may be interpreted as BR($\tilde{t}_1 \to eb$) or BR($\tilde{t}_1 \to \mu b$).

It is expected that the invariant mass of the lepton and jet should show a peak at $m_{\tilde{t}_1}$. However, a combinatorial problem arises when the decay of a pair of $\tilde{t}_1$ is considered. The last kinematic selection 8 is used to reconstruct the top

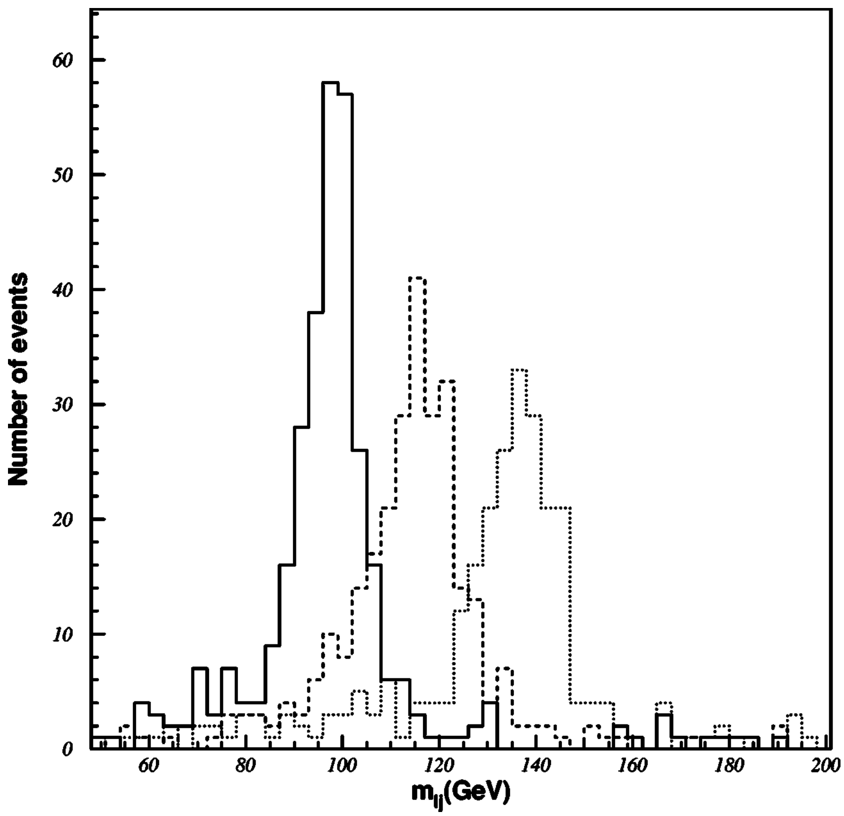

FIG. 2. The lepton-jet invariant mass ($m_{\ell j}$) distribution for $\mathcal{L}=2$ fb^{-1}, for three top squark masses 100 GeV (solid line), 120 GeV (dashed line), and 140 GeV (dotted line).

squark mass. The correct lepton-jet combination can be separated out by demanding that the difference between any two lepton-jet invariant masses ($m_{\ell j}$) be the minimum. In Fig. 2 we show the lepton-jet invariant mass distribution normalized for $\mathcal{L}=2$ fb^{-1} and with $\epsilon_{br}=1$ and for three $m_{\tilde{t}_1}$ masses, 100, 120, and 140 GeV which are presented by solid, dashed, and short-dashed lines, respectively. We have not shown the corresponding distributions for any of the backgrounds since after imposing all cuts they turn out to be negligible (see Table I). As expected, visible peaks at each $m_{\tilde{t}_1}$ is present which are not expected in any of the backgrounds. Therefore, in this channel, the mass of $\widetilde{t_1}$ can be measured with reasonable accuracy. More importantly the successful reconstruction of the top squark mass unambiguously implies that the lepton number violating nature of the interaction underlying $\widetilde{t_1}$ decays. The actual signal size may be considerably larger due to reasons discussed above. Thus the possibility that the reach will extend to higher $m_{\tilde{t}_1}$ or smaller ϵ_{br} is therefore quite open.

IV. STOP DECAY BRANCHING RATIOS AND LIMITS ON λ' IN MODELS OF m_ν

As mentioned in the Introduction, when $\tilde{t}_1$ is the NLSP in RPV models of ν mass, three decay channels are allowed, which may naturally compete with each other in various regions of the MSSM parameter space. They are the loop induced flavor changing decay mode, Eq. (5) [22], the four-body decay into states with nearly massless fermions, the bottom quark and the LSP, Eq. (6) [27,35], and the RPV decay mode Eq. (1). In this section we discuss the systematics of MSSM parameter space which enable us to identify the regions where different decay modes dominate.

If the sleptons are lighter than $\tilde{t}_1$, then the three-body decay mode, Eq. (3), involving sleptons opens up. The competition between $\tilde{t}_1 \to b\ell\tilde{\nu}$ and $\tilde{t}_1 \to b\tilde{\ell}\nu$ and the RPV mode has been discussed in Ref. [19]. Here we shall also identify regions of the parameter space where the decay modes given by Eqs. (1), (3), and (5) compete with each other and demarcate the difficult regions for top squark search at Run-II where all decay modes may have relatively low rates.

It has been mentioned earlier that the couplings λ'_{i33} are the most important ones in models of m_ν. In Ref. [16] the upper bounds on these couplings were obtained from neutrino data in a variety of scenarios. In all cases the bounds were found to be approximately of the same order of magnitude ($\sim 10^{-3}$–10^{-4}). Our analysis based on the limiting BR of the last section can estimate the constraints on λ'_{13j} or λ'_{23j} obtainable from Run-II data. As before we shall assume only one of these couplings to be dominating and shall henceforth drop the index of λ'.

For our analysis we fix the parameters, which are required to calculate the ϵ parameter [see Eq. (12)]: (i) The *CP*-odd neutral higgs mass $M_A=300$ GeV, (ii) the trilinear coupling in the sbottom sector $A_b=300$ GeV, and (iii) the trilinear coupling in the stau sector $A_\tau=200$ GeV. The variation of the BR with respect to the other parameters will be explicitly discussed as and when required.

A. Competition between the loop induced and RPV decays

As is well known the loop decay width is controlled by the parameter ϵ which denotes the amount of $\tilde{t}_{L,R}$-$\tilde{c}_L$ mixing [22] and enters in the decay width,

$$\Gamma(\tilde{t}_1\to c\tilde{\chi}_1^0)=\frac{\alpha}{4}|\epsilon|^2 f^2 m_{\tilde{t}_1}\left(1-\frac{m^2_{\tilde{\chi}_1^0}}{m^2_{\tilde{t}_1}}\right)^2, \tag{12}$$

where f is the composition of neutralino mixing. The detailed expressions for ϵ and the function f can be found in Refs. [22,27]. Neglecting the lepton and the light quark masses the decay width of the channel $\tilde{t}_1\to l^+ d$ ($l=e$ or μ) is

$$\Gamma_{R\!\!\!/}=\frac{1}{16\pi}\lambda'^2 m_{\tilde{t}_1}\cos^2\theta_{\tilde{t}}, \tag{13}$$

where λ' is the dominant RPV coupling and $\theta_{\tilde{t}}$ is the mixing angle in the top squark sector.

As long as the two-body and three-body RPC decay modes Eqs. (2) and (3) do not open up, i.e., if the top squark is the NLSP, the above two modes compete with each other. In principle the four-body decay mode could also enter into the competition. However, in order to study the simplest example of competing modes the latter has been suppressed by considering relatively large values of $\tan\beta$ [35]. The competition among all three decay modes will be considered later.

If λ' is close to its current experimental bound from indirect searches [17], then the RPV decay dominates over the loop decay for the entire region of the parameter space unless $\cos\theta_{\tilde{t}}$ is fine tuned to be very small. The competition between the two modes becomes generic when λ' is $\sim 10^{-3}$–10^{-4}, which is interesting from the point of view of RPV models of neutrino mass [15,16]. The estimate $\lambda' \sim 10^{-4}$, as mentioned in the Introduction, is based on the assumption that the SUSY breaking scale (M_{SUSY}) ~ 100 GeV [16]. Somewhat larger values of M_{SUSY} push this estimate upwards. On the other hand, values of λ' somewhat smaller than $\sim 10^{-4}$ may be relevant if the absolute values of the neutrino masses, which are not known at the moment, are much smaller than the typical choice ~ 1 eV.

As we know, M_2, the SU(2) gaugino mass parameter (gaugino mass unification is assumed), μ, the higgsino mass parameter, and $\tan\beta$, the ratio of two vacuum expectation values of higgs sector, completely describe the neutralino and the chargino sector. We have chosen these parameters such that the $m_{\tilde{\chi}^\pm}$ is around 200 GeV, which more or less fixes the limit of the top squark mass up to which the competition among various decay channels can occur. Otherwise the two-body decay mode of $\tilde{t}_1$, Eq. (2), will open up and dominate over all other decay modes. The common slepton mass is taken to be heavier than $m_{\tilde{t}_1}$ to avoid the three-body decay channel.

In Fig. 3 the competition between these two decay mode has been illustrated for various values of $m_{\tilde{t}_1}$. The other MSSM parameters involved in this calculation are: $M_2 = 250$ GeV, $\mu = +250$ GeV, $\tan\beta = 40$, the common scalar squark mass $m_{\tilde{q}} = 300$ GeV, common slepton mass $m_{\tilde{\ell}} = 235$ GeV, $\cos\theta_{\tilde{t}} = 0.7$, and $\lambda' = 0.001$.

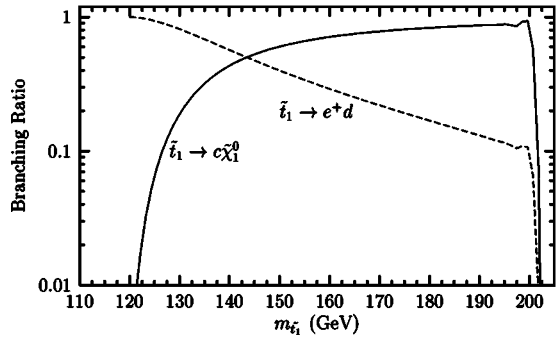

FIG. 3. The RPV and loop decay BR's as functions of $m_{\tilde{t}_1}$. The other MSSM parameters are $M_2 = 250$ GeV, $\mu = +250$ GeV, $\tan\beta = 40$, $m_{\tilde{q}} = 300$ GeV, $m_{\tilde{\ell}} = 235$ GeV, $\cos\theta_{\tilde{t}} = 0.7$, and $\lambda' = 0.001$.

As the top squark mass is increased, the ϵ parameter as well as the phase space factor $(1-m^2_{\tilde{\chi}_1^0}/m^2_{\tilde{t}_1})^2$ in Eq. (12) increase, but the former rises more sharply. Although both the widths in Eqs. (12) and (13) have a common linear dependence on $m_{\tilde{t}_1}$, the loop decay BR dominates over that of the RPV decay above a certain $m_{\tilde{t}_1}$. This happens for almost all choices of the other parameters, unless they are fine tuned to make ϵ very small.

For smaller value of $\cos\theta_{\tilde{t}}$, both the loop and RPV decay widths decrease, the former through the ϵ term and the latter through the direct dependence on $\cos\theta_{\tilde{t}}$, respectively. The competition between the two BR's still occur albeit for higher top squark masses. The competition ceases to exist only if $\cos\theta_{\tilde{t}}$ is fine tuned to make the ϵ parameter negligible.

The RPV decay width depends on the product $\lambda'\cos\theta_{\tilde{t}}$. Keeping this product [i.e., the width in Eq. (13)] fixed, if we increase λ', the loop decay width will decrease as a consequence of lowering $\cos\theta_{\tilde{t}}$. So, the competition will take place for higher top squark masses only. However, above a certain λ' the loop decay fails to compete for the entire range of $m_{\tilde{t}_1}$ corresponding to a top squark NLSP. On the other hand, for smaller λ' the RPV decay width is scaled down in a straight forward way. Now the competition occurs over a larger range of $m_{\tilde{t}_1}$ and for smaller values of $\cos\theta_{\tilde{t}}$ and/or $\tan\beta$.

If $\tan\beta$ is lowered, for fixed μ and M_2, the chargino mass is lowered by a small amount so that the threshold for the two-body decay is slightly lowered. More importantly, the ϵ parameter decreases dramatically below a certain $\tan\beta$. Here the RPV decay overwhelms the loop decay. However, precisely for such low values of $\tan\beta$ the four-body decay become important if, in addition, the chargino is of low virtuality ($m_{\tilde{t}_1}\approx m_{\tilde{\chi}^\pm}$; see the next subsection).

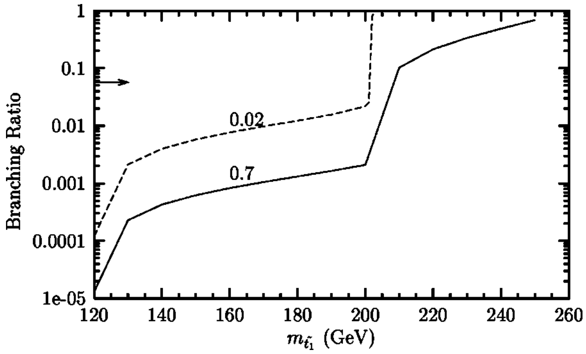

FIG. 4. The minimum value of λ' at 5σ for observable signal for $\cos\theta_{\tilde{t}}$=0.7 (solid) and 0.02 (dashed curve), the other parameters are same as in Fig. 3.

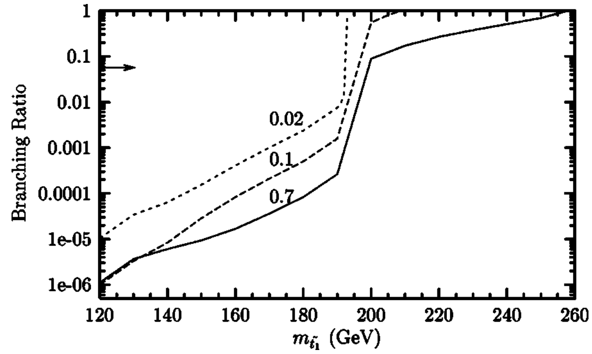

FIG. 6. The minimum value of λ' at 5σ for observable signal for $\cos\theta_{\tilde{t}}$=0.7 (solid), 0.1 (dashed), and 0.02 (dotted curve). The other MSSM parameters are the same as in Fig. 5.

Even if λ' is as low as $\sim 10^{-4}$ the competition between the two modes still exists for smaller values of $\tan\beta$ which lowers ϵ and hence the loop decay width. The minimum value of BR, as shown in Fig. 1, can be used to find the limiting value of λ' considering Eqs. (12) and (13). In Fig. 4 the two curves represent limiting values of λ' for observable signal for two values of $\cos\theta_{\tilde{t}}$. The regions above the curves correspond to observable BR as given in Fig. 1. The other SUSY parameters chosen are as in Fig. 3. In this figure and the similar ones presented subsequently, the horizontal arrow represents the upper bound on λ'_{131} obtained prior to the neutrino data [17]. The bounds on λ'_{132} and λ'_{23j} are even weaker. Only the bound on λ'_{133} is $\sim 10^{-3}$. Hence significant improvement in the existing limits on many RPV couplings is expected. For larger $\cos\theta_{\tilde{t}}$, the RPV decay width increases significantly. As a result the BR constraint is satisfied for lower λ'. The sharp rise in the curve for $m_{\tilde{t}_1} \gtrsim 200$ GeV is a consequence of the opening up of the two-body channel $\tilde{t}_1 \to b\tilde{\chi}_1^{\pm}$. It is interesting to note that for large $\cos\theta_{\tilde{t}}$ the data will be sensitive to the values of λ' relevant for neutrino masses until the two-body decay channel opens up.

B. Competition between the four-body and RPV decay

The dependence of the four-body decay rate on supersymmetric parameters has been discussed in great detail in Refs. [27,35]. The competition between four-body decay modes with the loop induced flavor changing decay mode, Eq. (5), has been discussed both in the MSSM and mSUGRA models in Ref. [35].

In general, the parameter space relevant for competition between the RPV decay channel and the four-body decay channel corresponds to almost right handed $\widetilde{t_1}$ (i.e., $\cos\theta_{\tilde{t}}$ small) and $\lambda' \sim 10^{-3}$ or 10^{-4}. For small value of $\tan\beta$, the loop decay amplitude becomes negligible. In Fig. 5 we demonstrate this competition for $\lambda' = 10^{-4}$ as a function of $m_{\tilde{t}_1}$. The choice of other MSSM parameters are mentioned in the figure caption.

As expected, the four-body decay channel opens up for relatively low mass difference $(m_{\tilde{t}_1} - m_{\tilde{\chi}_1^{\pm}})$ so that the chargino in the four-body decay process has a small virtuality. In Fig. 6 we show the range of λ' which can be probed by Run-II experiments for a given set of MSSM parameters chosen for Fig. 5.

C. Competition between the loop, four-body, and RPV decay

In order to illustrate the possibility of competition among all three channels, we shall keep in mind that the ϵ parameter must not be as small as in the previous section. The competition is demonstrated in Fig. 7 with the choice of SUSY parameters mentioned in the figure caption.

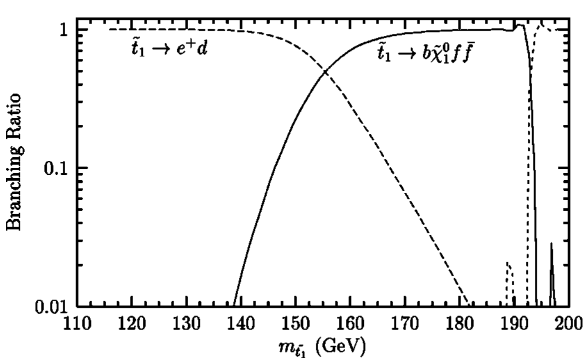

FIG. 5. The RPV and four-body decay BR's are shown. The other MSSM parameters are $M_2 = 250$ GeV, $\mu = +250$ GeV, $\tan\beta = 6$, $m_{\tilde{q}} = 300$ GeV, $m_{\tilde{\ell}} = 210$ GeV, $\cos\theta_{\tilde{t}}$=0.1, and $\lambda' = 0.0001$.

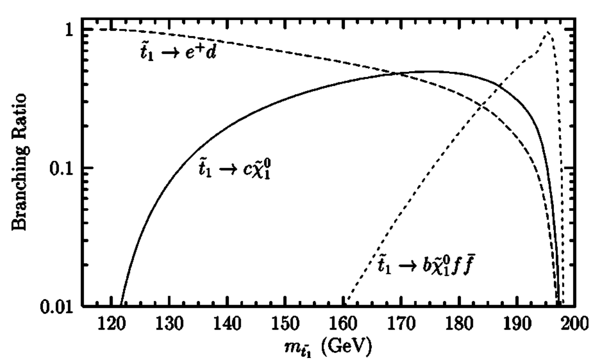

FIG. 7. The RPV, loop and four-body decay BR's are shown. The other MSSM parameters are $M_2 = 250$ GeV, $\mu = +250$ GeV, $\tan\beta = 10$, $m_{\tilde{q}} = 300$ GeV, $m_{\tilde{\ell}} = 210$ GeV, $\cos\theta_{\tilde{t}}$=0.9, and $\lambda' = 0.0001$.

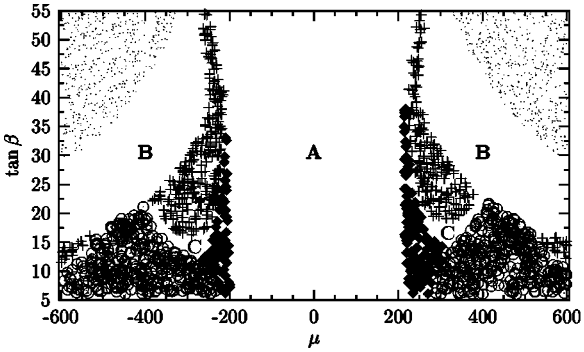

FIG. 8. Different regions dominated by a particular decay channel of top squark are shown for $m_{\tilde{t}_1}=180$ GeV. See the text for conventions for demarcating regions. Except for $\cos\theta_{\tilde{t}}=0.3$, all the other parameters are same as in Fig. 7.

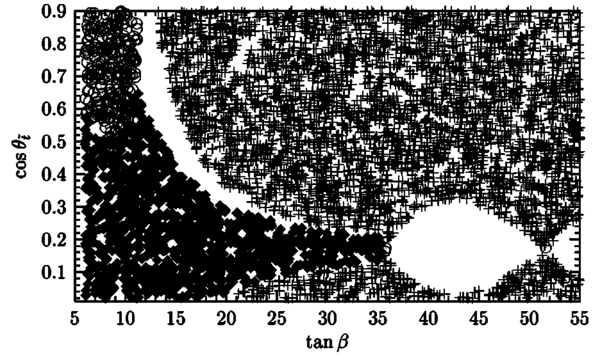

FIG. 9. Similar information as is in Fig. 8 for the same set of MSSM parameters as in Fig. 7, except for $\mu=250$ GeV.

The total four-body BR's is significant ($\gtrsim 10\%$) for the range, $m_{\tilde{\chi}_1^\pm}-20 \lesssim m_{\tilde{t}_1} \lesssim m_{\tilde{\chi}^\pm}$. In this top squark mass range the chargino is of very small virtuality. Also we choose $m_{\tilde{\ell}}$, the common slepton mass, such that even after mixing the lighter tau slepton mass $m_{\tilde{\tau}_1}$ is above the chargino mass. So the slepton mediated four-body process also has a low virtuality, yet the three-body decay mode, Eq. (3), is kinematically forbidden.

If the signal is seen in all three channels then one has to identify the region of the parameter space where the corresponding BR's are above the observable limit. Similarly, in order to exclude a particular $m_{\tilde{t}_1}$ comprehensively it is essential to establish that at least one of the competing modes would be observable over the entire parameter space. In order to do a complete job one needs the minimum observable BR's at Run-II for each of the allowed modes. Unfortunately at the moment we have numerical estimates for the RPV mode ($\tilde{t}_1 \rightarrow e^+ d_j$) only (see Fig. 1). In the following we shall delineate the regions of the parameter space where (i) the RPV decay rate is observable at Run-II or (ii) one of the two competing RPC modes have a sizable BR.

The relevant information will be presented in the form of scatter plots obtained by varying two important parameters randomly keeping the others fixed. The scatter plots also illustrate the competition among the decay modes in specific regions of the parameter space.

In Fig. 8, fixing $m_{\tilde{t}_1}=180$ GeV, $\cos\theta_{\tilde{t}}=0.3$, μ and $\tan\beta$ are varied randomly setting the other parameters as in Fig. 7. The fixing of $m_{\tilde{t}_1}$, which tacitly assumes that $m_{\tilde{t}_1}$ can be reconstructed, makes the analysis simpler. The systematics of the parameter space is clear from Fig. 8. In this figure, the region marked by circles is the one where the RPV mode is above the observable limit, i.e., $\mathrm{BR}(\tilde{t}_1 \rightarrow e^+ + d) \gtrsim 26\%$ (see Fig. 1). Although the width of this mode does not depend upon μ or $\tan\beta$ directly, its BR is quite sensitive to these parameters. The regions marked by "**+**" correspond to $\mathrm{BR}(\tilde{t}_1 \rightarrow c\tilde{\chi}_1^0) \gtrsim 75\%$ and those marked by the black diamonds correspond to $\mathrm{BR}(\tilde{t}_1 \rightarrow b\tilde{\chi}_1^0 f\overline{f'}) \gtrsim 30\%$ with the RPV BR less than the observable limit. Note that for low values of $\tan\beta$, the RPV BR is much larger than 30%. In the region labeled by "**A**," $m_{\tilde{t}_1} > m_{\tilde{\chi}^\pm} + m_b$, the two-body decay mode, Eq. (2), opens up and overwhelms all other decay channels. Finally, the region marked by "**B**," where μ and $\tan\beta$ are large, the lighter tau slepton mass eigenstate ($\tilde{\tau}_1$) becomes rather light and the three-body decay mode involving a $\tilde{\tau}_1$ in the final state strongly dominates. In the dotted region $\tilde{\tau}_1$ is lighter than the $\tilde{\chi}_1^0$ or has unphysical mass. Although $m_{\tilde{\tau}_1} \lesssim m_{\tilde{\chi}_1^0}$ is allowed in RPV MSSM in general, we have not investigated top squark signals in this scenario.

If the top squark signal is seen in one or more channels then one can broadly identify the relevant region of the parameter space. For example, if all three modes are seen then the white region ("**C**") or regions in its neighborhood could be of interest. For more precise conclusions one needs to know the limiting BR of all the modes quantitatively. One can hope that Tevatron Run-II and/or LHC will gradually supply the relevant information. However, the same region may be difficult to exclude at Run-II even if no signal is seen, since in parts of this region all the BR's may turn out to be below the observable limit.

In Fig. 9 the scatter plot is in the $\tan\beta-\cos\theta_{\tilde{t}}$ plane with $\mu=250$ GeV and the other parameters as in Fig. 7. The convention for demarcating the regions are also the same as in Fig. 8. Again the white regions could be the difficult ones

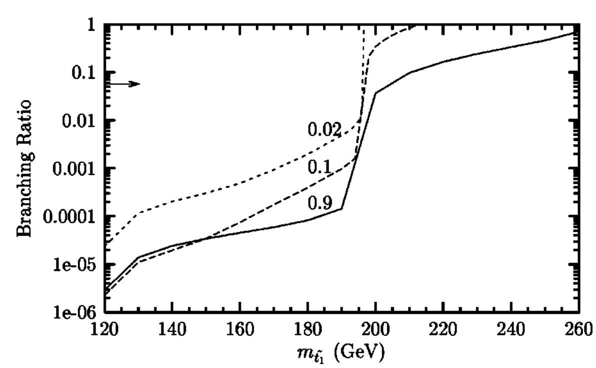

FIG. 10. Similar information as in Fig. 6, for $\cos\theta_{\tilde{t}}=0.9$ (solid), 0.1 (dashed), and 0.02 (dotted curve). Other parameters are the same as in Fig. 7.

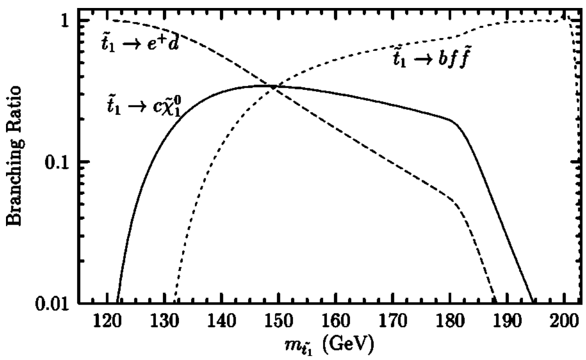

FIG. 11. The RPV, loop and three-body decay BR's as functions of $m_{\tilde{t}_1}$. The other MSSM parameters are $M_2 = 250$ GeV, $\mu = +250$ GeV, $\tan\beta = 40$, $m_{\tilde{q}} = 300$ GeV, $m_{\tilde{\ell}} = 175$ GeV, $\cos\theta_{\tilde{t}} = 0.5$, and $\lambda' = 0.001$.

from the point of view of comprehensive $\widetilde{t_1}$ search at Run-II.

In Fig. 10 the three curves represent limiting values of λ' for the observable signal for three values of $\cos\theta_{\tilde{t}}$. The regions above the curves correspond to the observable BR as given in Fig. 1. The other SUSY parameters chosen are the same as in Fig. 7. It is interesting to note that for large $\cos\theta_{\tilde{t}}$ the data will be sensitive to values of λ' relevant for neutrino masses until the two-body decay channel opens up. It is to be noted that for relatively small $m_{\tilde{t}_1}$ the bound is fairly insensitive to $\cos\theta_{\tilde{t}}$ for the range $0.1 \lesssim \cos\theta_{\tilde{t}} \lesssim 0.9$. As the threshold of the four-body decay opens up for larger $m_{\tilde{t}_1}$, the constrain on λ' gets weaker as expected.

D. Competition between the three-body, loop, and RPV decay

The competition between the RPV decay mode, the loop decay, and all RPC three-body channels has been studied in Ref. [39]. In this section we consider a scenario where the top squark is not the NLSP and the first two RPC decay modes of Eq. (3) are open. We then study the competition among these two modes, the loop decay and the RPV decay, taking into account the limiting BR of the last mode obtained in Sec. III. As the three-body decay mode is kinematically allowed for light sleptons only, the slepton mass should be chosen with care so that it is consistent with the experimental lower limit.

With the choice of the SUSY parameters as in Fig. 11, the three-body decays, if kinematically allowed, have BR $\gtrsim 10\%$ almost for the entire range of top squark masses. For this set of parameters, the $m_{\tilde{\tau}_1}$, $m_{\tilde{\nu}}$, and $m_{\tilde{\ell}}$ ($\ell = e$ or μ) are 124 GeV, 156 GeV, and 175 GeV, respectively.

Interestingly, we have found that when the chargino is in the mixed region with a relatively large mass, i.e., when the three-body decay width is somewhat reduced both due to a mixing angle factor and propagator suppression, there may be a competition among the loop, three-body decay, and RPV decay modes for $\lambda' = 0.001$. Here the loop decay width is significant thanks to relatively large $\cos\theta_{\tilde{t}} = 0.5$ and large $\tan\beta$. This is demonstrated in Fig. 11. It follows from Fig. 11 that in the neighborhood of $m_{\tilde{t}_1} = 150$ GeV all three modes coexist with nearly equal BR. However, from the limiting BR plot (see Fig. 1) we find that in this region the signal is observable if $\mathrm{BR}(\tilde{t}_1 \to e^+ + d) \gtrsim 20\%$. Hence the loop decay channel may not be very important as the discovery channel. If the $\mathrm{BR}(\tilde{t}_1 \to e^+ + d)$ is below the observable limit, the three-body mode will be the main discovery channel. In Fig. 11, for relatively low $m_{\tilde{t}_1}$, the three-body mode with $\tilde{\tau}_1$ in the final state opens up. For higher $m_{\tilde{t}_1}$ the modes with $\tilde{\nu}$ and other sleptons in the final state are also allowed.

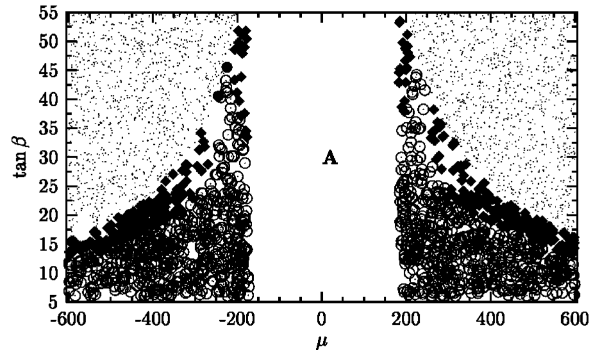

FIG. 12. Similar information as in Fig. 8, but for $m_{\tilde{t}_1} = 160$ GeV. The other parameters are the same as in Fig. 11.

In Fig. 12, the competition among the three decay modes is illustrated in the $\mu - \tan\beta$ plane, for $m_{\tilde{t}_1} = 160$ GeV. For this $m_{\tilde{t}_1}$ only the three-body mode with $\tilde{\tau}_1$ in the final state is relevant. In Fig. 12 the dotted circles delineate the parameter space where the RPV decay is observable. The regions characterized by relatively large μ and $\tan\beta$ correspond to the light $\tilde{\tau}_1$ scenario. This part of the parameter space is dominated by the three-body decays (the black diamonds correspond to BR $\gtrsim 70\%$). The dotted region is theoretically disfavored as explained in the context of Fig. 8. Finally, the black circles represent the parameter space with $40\% \lesssim \mathrm{BR}(\tilde{t}_1 \to c\tilde{\chi}_1^0) \lesssim 70\%$. Only a few points appear at large $\tan\beta$. In the region marked by "**A**" the two-body decay mode overwhelms the other modes. In Fig. 13 a scatter plot is presented in the $\tan\beta - \cos\theta_{\tilde{t}}$ plane following the same convention. The region "**C**" is the difficult region with no clearly dominating BR.

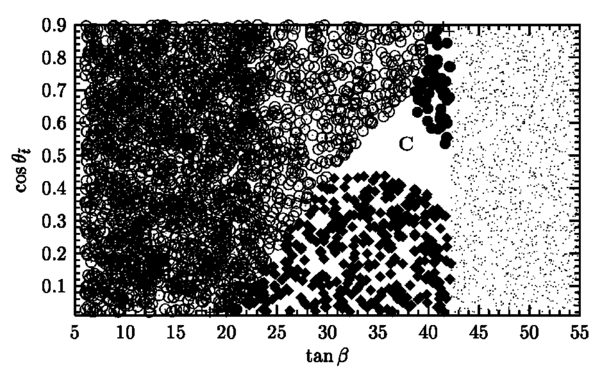

FIG. 13. Similar information as in Fig. 12 using different variables.

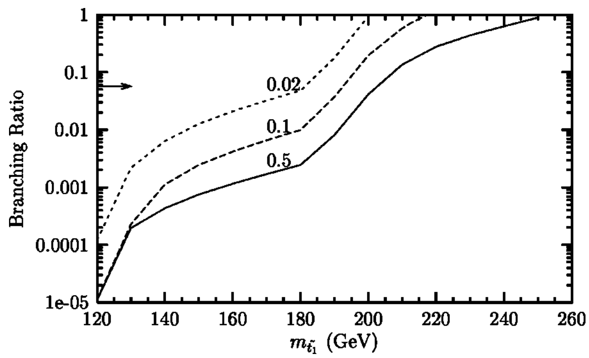

FIG. 14. Similar information as in Fig. 6 for cos $\theta_{\tilde{t}}$=0.5 (solid), 0.1 (dashed), and 0.02 (dotted curve) and the other parameters are the same as in Fig. 11.

In Fig. 14 we present the limiting value of λ' for three values of cos $\theta_{\tilde{t}}$ corresponding to the parameter space of Fig. 11. The first change in the slope occurs at about $m_{\tilde{t}_1}=130$ GeV due to the opening up of the channel $\tilde{t}_1 \to b \nu_\tau \tilde{\tau}_1$. The second change in the neighborhood of $m_{\tilde{t}_1}=180$ GeV corresponds to the decay mode $\tilde{t}_1 \to b \nu_l \tilde{\ell}$ ($\ell = e$ or μ). In both cases the BR's of the RPV decay mode are reduced which have to be compensated by higher values of λ'. Finally for $m_{\tilde{t}_1} \gtrsim 210$ GeV, the two-body decay channel, Eq. (2), becomes the main decay mode.

V. CONCLUSION

It is quite possible that the mass of the lighter top squark is much smaller than the other squarks and gluinos due to mixing and RG effects and it is likely to be the only strongly interacting superparticle within the kinematic reach of Run-II of the Tevatron with a large production cross section. If this is the case then the direct RPV decay $\tilde{t}_1 \to l_i^+ d_j$ driven by the trilinear couplings λ'_{i3j}, where *i* and *j* are generation indices, may be the most attractive channel for discovering *R*-parity violation [18–20].

Additional interest in this process stems from the fact that some subset of the above couplings, in particular λ'_{i33}, may be important ingredients of RPV models of ν mass [15,16]. This scenario constrains the magnitudes of these couplings to be generically small ($\lesssim 10^{-3}$–10^{-4}, see, e.g., Ref. [16]).

If the couplings are indeed so small the RPC two-body decay, Eq. (2), or three-body decay modes, Eq. (3), if kinematically allowed, would overwhelm the RPV decay and the LSP decay may be the only signature of *R*-parity violation [25]. The signature, Eq. (4), however, may not reveal the lepton number violating nature of the underlying interaction or whether the strength of the coupling is indeed in the right ballpark required by models of ν mass.

The situation is dramatically different if the $\tilde{t}_1$ be the NLSP, since the allowed RPC decays—the loop induced, Eq. (5), or the four-body channel, Eq. (6)—are naturally suppressed. If the RPV coupling is indeed $\sim 10^{-3}$–10^{-4} then BR's of the three allowed channels may indeed be comparable. Thus the simultaneous observation of two or more of these decays may be a hallmark of RPV models of m_ν.

In Sec. III using the event generator PYTHIA [21] we have estimated the minimum value of the BR of the RPV decay channel $\tilde{t}_1 \to e^+ d_j$ for various values of $m_{\tilde{t}_1}$ corresponding to observable signals at Run-II experiments. Our results (see Fig. 1) show that much smaller BR's can be probed at Run-II with 2 fb^{-1} of data compared to the bounds obtained from Run-I data [20]. These results are approximately valid also for the channel $\tilde{t}_1 \to \mu^+ d_j$. In reality, the limiting BR may be much smaller than our conservative estimates as can be seen by using an enhanced NLO cross section [31], larger integrated luminosity, or by employing *b* tagging to improve the $S/sqrtB$ ratio, since in many models λ'_{i33} are the most important couplings. Our simulations show that $m_{\tilde{t}_1}$ can be reconstructed from the decay products with reasonable accuracy, revealing thereby the lepton number violating nature of the underlying decay dynamics.

It is gratifying to note that even our conservative estimates of the limiting BR can be translated into interesting upper bounds on the RPV couplings λ'_{i3j} ($i=1$ or 2) for representative choices of the MSSM parameters if no signal is seen (see Figs. 4, 6, 10, 14). Thus the existing bounds [17] on several λ'_{i3j} (except perhaps λ'_{133}) can be significantly improved if no signal is seen. These results indicate that the Run-II data will indeed be sensitive to magnitudes of these couplings even if they are as small as that required by the models of m_ν.

Using our estimate of the limiting BR as a function of $m_{\tilde{t}_1}$ one can demarcate the regions of the MSSM parameter space in specific models, where the RPV decay is observable. In Sec. IV we have also studied the systematics of the MSSM parameter space and have delineated the regions where the competing decay modes are numerically significant. One can also have some idea of the difficult regions of the parameter space where the BR of none of the competing decays clearly dominates. All this information will become more precise once full simulations of the competing channels [Eqs. (7) and (8)] estimate the limiting BR's corresponding to all signals. If no signal is seen then the program for top squark search at the LHC may focus on the regions of the parameter space which were difficult in Run-II experiments.

ACKNOWLEDGMENTS

A.D. acknowledges financial support from BRNS (India) under Project No. 2000/37/10/BRNS. S.P.D. acknowledges a grant by CSIR, India. He also thanks N. K. Mondal and members of the DHEP group for supporting a visit at the Tata Institute of Fundamental Research where part of this work was done.

[1] For reviews of supersymmetry, see, e.g., H.P. Nilles, Phys. Rep. **1**, 110 (1984); H.E. Haber and G. Kane, *ibid.* **117**, 75 (1985); M. Drees and S. P. Martin, CLTP Report (1995); hep-ph/9504324.

[2] See, e.g., ALEPH Collaboration, Phys. Lett. B **544**, 73 (2002), and references therein; for a summary, see http://lepsusy.web.cern.ch/lepsusy

[3] CDF Collaboration, T. Affolder *et al.*, Phys. Rev. Lett. **88**, 041801 (2002), and references therein.

[4] For a summary of Run-I results, see, e.g., S. Abel *et al.*, report of the SUGRA working group for ''Run-II at the Tevatron,'' hep-ph/0003154, and references therein.

[5] J. Ellis and S. Rudaz, Phys. Lett. **128B**, 248 (1983); M. Drees and K. Hikasa, Phys. Lett. B **252**, 127 (1990).

[6] M. Carena, M. Quiros, and C.E. Wagner, Phys. Lett. B **380**, 81 (1996); Nucl. Phys. **B503**, 387 (1997); **B524**, 3 (1998); D. Delepine, J.M. Gerard, R. Gonzalez Felipe, and J. Weyers, Phys. Lett. B **386**, 183 (1996); J. McDonald, *ibid.* **413**, 30 (1997); J.M. Cline and G.D. Moore, Phys. Rev. Lett. **81**, 3315 (1998).

[7] L.J. Hall and M. Suzuki, Nucl. Phys. **B231**, 419 (1984).

[8] L. Ibanez and G.G. Ross, Phys. Lett. B **260**, 291 (1992).

[9] For a review, see, e.g., H. Dreiner, in *Perspectives on supersymmetry*, edited by G. L. Kane, hep-ph/9707435 (World Scientific, in press).

[10] For a review of collider signatures of RPV, see, e.g., *Report of the Group on R-parity Violation*, R. Barbieri *et al.*, hep-ph/9810232; B. Allanach *et al.*, report of the working group for ''Searching for R-parity violation at Run-II of Tevatron,'' hep-ph/9906224.

[11] H. Baer, C. Kao, and X. Tata, Phys. Rev. D **51**, 2180 (1995); M. Guchait and D.P. Roy, *ibid.* **54**, 3276 (1996); F. Borzumati, R.M. Godbole, J.L. Kneur, and F. Takayama, J. High Energy Phys. **07**, 037 (2002), and references therein.

[12] C.S. Aulakh and R.N. Mohapatra, Phys. Lett. B **119**, 136 (1982); L. Hall and M. Suzuki, Nucl. Phys. **B231**, 419 (1984); J. Ellis *et al.*, Phys. Lett. **150B**, 142 (1985); G. Ross and J. Valle, *ibid.* **151B**, 375 (1985); S. Dawson, Nucl. Phys. **B261**, 297 (1985).

[13] Super-Kamiokande Collaboration, Y. Fukuda *et al.*, Phys. Rev. Lett. **81**, 1562 (1998).

[14] SNO Collaboration, Q.R. Ahmed *et al.*, Phys. Rev. Lett. **89**, 011301 (2002); **89**, 011302 (2002).

[15] M. Nowakowski and A. Pilaftsis, Nucl. Phys. **B461**, 19 (1996); A.Y. Smirnov and F. Vissani, *ibid.* **B460**, 37 (1996); J. Valle, hep-ph/9712277; B. Mukhopadhyaya, S. Roy, and F. Vissani, Phys. Lett. B **443**, 191 (1998); M. Drees, S. Pakvasa, X. Tata, and T. ter Veldhuis, Phys. Rev. D **57**, 5335 (1998); S. Rakshit, G. Bhattacharyya, and A. Raychaudhuri, *ibid.* **59**, 091701 (1999); S.Y. Choi, E.J. Chun, S.K. Kang, and J.S. Lee, *ibid.* **60**, 075002 (1999); A.S. Joshipura and S. Vempati, *ibid.* **60**, 111303 (1999); S. Davidson and M. Losada, J. High Energy Phys. **05**, 021 (2000); T.F. Feng and X.Q. Li, Phys. Rev. D **63**, 073006 (2001); Y. Koide and A. Ghosal, hep-ph/0203113; I. Gogoladze and A. Perez-Lorenzana, Phys. Rev. D **65**, 095011 (2002); R. Adhikari, A. Sil, and A. Raychaudhuri, Eur. Phys. J. C **25**, 125 (2002); F. Borzumati and J.S. Lee, Phys. Rev. D **66**, 115012 (2002); G. Bhattacharya, hep-ph/0305330, and references therein.

[16] A. Abada and M. Losada, Phys. Lett. B **492**, 310 (2000).

[17] V. Barger, G.F. Giudice, and T. Han, Phys. Rev. D **40**, 2987 (1989); G. Bhattacharyya, hep-ph/9709395; B.C. Allanach, A. Dedes, and H.K. Dreiner, Phys. Rev. D **60**, 075014 (1999).

[18] Aseshkrishna Datta and Biswarup Mukhopadhyaya, Phys. Rev. Lett. **85**, 248 (2000).

[19] D. Restrepo, W. Porod, and J.W.F. Valle, Phys. Rev. D **64**, 055011 (2001).

[20] Subhendu Chakrabarti, M. Guchait, and N.K. Mondal, Phys. Rev. D **68**, 015005 (2003).

[21] T. Sjostrand, P. Eden, C. Friberg, L. Lonnblad, G. Miu, S. Mrenna, and E. Norrbin, Comput. Phys. Commun. **135**, 238 (2001).

[22] K.I. Hikasa and M. Kobayashi, Phys. Rev. D **36**, 724 (1987).

[23] A. Bartl, W. Majerotto, B. Mosslacher, N. Oshimo, and S. Stippel, Phys. Rev. D **43**, 2214 (1991); H. Baer, M. Drees, R. Godbole, J.F. Gunion, and X. Tata, *ibid.* **44**, 725 (1991).

[24] W. Porod and T. Wohrmann, Phys. Rev. D **55**, 2907 (1997); **67**, 059902(E) (2003).

[25] V. Barger, T. Han, S. Hasselbach, and D. Marfatia, Phys. Lett. B **538**, 346 (2002).

[26] W. Porod *et al.*, Phys. Rev. D **63**, 115004 (2001); M.B. Magro *et al.*, J. High Energy Phys. **09**, 071 (2003).

[27] C. Boehm, A. Djouadi, and Y. Mambrini, Phys. Rev. D **61**, 095006 (2000); A. Djouadi and Y. Mambrini, *ibid.* **63**, 115005 (2001).

[28] H1 Collaboration, C. Adloff *et al.*, Z. Phys. C **74**, 191 (1997); ZEUS Collaboration, J. Breitweg *et al.*, *ibid.* **74**, 207 (1997).

[29] M. Guchait and D.P. Roy, Phys. Rev. D **57**, 4453 (1998).

[30] D.P. Roy, Phys. Lett. B **283**, 270 (1992).

[31] W. Beenakker, M. Kramer, T. Plehn, M. Spira, and P.M. Zerwas, Nucl. Phys. **B515**, 3 (1998).

[32] H. Baer, J. Sender, and X. Tata, Phys. Rev. D **50**, 4517 (1994); J.L. Lopez, D.V. Nanopoulos, and A. Zichichi, Mod. Phys. Lett. A **10**, 2289 (1995); J. Sender, Phys. Rev. D **54**, 3271 (1996); Aseshkrishna Datta, M. Guchait, and K.K. Jeong, Int. J. Mod. Phys. A **14**, 2239 (1999).

[33] A. Djouadi, M. Guchait, and Y. Mambrini, Phys. Rev. D **64**, 095014 (2001).

[34] R. Demina, J. Lykken, K. Matchev, and A. Nomerotski, Phys. Rev. D **62**, 035011 (2000); M. Carena, D. Choudhury, R.A. Diaz, H.E. Logan, and C.E.M. Wagner, *ibid.* **66**, 115010 (2002).

[35] S.P. Das, Amitava Datta, and M. Guchait, Phys. Rev. D **65**, 095006 (2002).

[36] D0 Collaboration, S. Abachi *et al.*, Phys. Rev. Lett. **76**, 2222 (1996); for a summary on top squark searches at the Tevatron, see CDF and D0 Collaborations, A. Savoy-Navarro, Report FERMILAB-CONF-99-281-E (Nov. 1999); L3 Collaboration, M. Acciarri *et al.*, Phys. Lett. B **445**, 428 (1999); CDF Collaboration, T. Affolder *et al.*, Phys. Rev. Lett. **84**, 5704 (2000); ALEPH Collaboration, R. Barnate *et al.*, Phys. Lett. B **488**, 234 (2000); OPAL Collaboration, G. Abbiendi *et al.*, *ibid.* **545**, 272 (2002); **548**, 258 (2002).

[37] CDF Collaboration, D. Acosta *et al.*, Phys. Rev. Lett. **92**, 051803 (2004).

[38] ALEPH Collaboration, R. Barate *et al.*, Eur. Phys. J. C **19**, 415 (2001).

[39] M.A. Diaz, hep-ph/9711435; hep-ph/9712213; J.C. Romão,

hep-ph/9712362; J.W.F. Valle, talk at PASCOS 98, hep-ph/9808292; J.C. Romao, M.A. Diaz, M. Hirsch, W. Porod, and J.W.F. Valle, Phys. Rev. D **61**, 071703 (2000); M. Hirsch, M.A. Diaz, W. Porod, J.C. Romao, and J.W.F. Valle, *ibid.* **62**, 113008 (2000).

[40] G. Kane and J.P. Leveille, Phys. Lett. **112B**, 227 (1982); P.R. Harrison and C.H. Llewellyn-Smith, Nucl. Phys. **B213**, 223 (1983); S. Dawson, E. Eichten, and C. Quigg, Phys. Rev. D **31**, 1581 (1985); E. Reya and D.P. Roy, *ibid.* **32**, 645 (1985); H. Baer and X. Tata, Phys. Lett. **160B**, 159 (1985).

[41] CTEQ Collaboration, H.L. Lai *et al.*, Phys. Rev. D **55**, 1280 (1997).